UNSYS digital

Journal of Instrumentation, Automation, and Systems

Monitoring of Land Deformation in Kanagawa Prefecture using GNSS and C-band Sentinel-1 -based Consecutive DInSAR

Katsunoshin Nishi[†], Josaphat Tetuko Sri Sumantyo[†], Masaaki Kawai[‡], Mirza Muhammad Waqar[§], Xiangping Chen[†]

[†]Center of Environmental Remote Sensing, Chiba University.

[‡]Mitsubishi Heavy Industries, Ltd, Japan.

[§]Lumir Inc, Republic of Korea.

Abstract— In Japan, precipitation has recently become more localized, concentrated, and intense. Extreme precipitation has caused a rapid land deformation, which results in ground water levels and loss of building stability. For the appropriate maintenance and renewal of infrastructure, including the design method of underground structures, the utilization of remote sensing technology which can always observe the ground deformation over a wide range with high accuracy is expected. This research presents the results of long-term continuous land deformation (subsidence or uplift) monitoring and using Global Navigation Satellite System (GNSS) and Consecutive Differential Interferometric Synthetic Aperture Radar (DInSAR) technique in Yokohama, Yokosuka and Miura cities, Kanagawa Prefecture, Japan. We adopted the Consecutive DInSAR method with the small spatial and short time baseline between satellites. The satellite data used thirty-three pairs of Sentinel-1 data in descending orbit from December 27, 2017 to November 17, 2020, and twenty-two Sentinel-1 data pairs in ascending orbit from June 26, 2019 to October 30, 2020. The validation of the SAR images used the daily coordinate values of the GNSS control point provided by the Geographical Survey Institute (GSI). As a result of the analysis, the estimated land displacement and GNSS data agreed well in Yokohama, Yokosuka, and Miura cities. The RMSEs in descending orbit of Yokohama, Yokosuka and Miura cities were found to be 0.41 cm, 0.49 cm, and 0.49 cm, respectively and the RMSEs in ascending orbit of Yokohama, Yokosuka and Miura cities were found to be 0.68 cm, 0.53 cm, and 0.58 cm, respectively, demonstrating its capability to analyze the land displacement monitoring over under different topographical conditions. In the future, this research result is expected to applicable in the field of disaster monitoring and environmental change observation which continuously require high accuracy observation over a wide area.

Keywords— Consecutive DInSAR; GNSS; Sentinel-1; Land Deformation; Kanagawa prefecture

DOI: 10.21535/zenodo.11530709

I. INTRODUCTION

TOKYO metropolitan area which is home to about 33% of the Japan's population[1] due to concentration of social and economic infrastructure is prone to disaster such as heavy rains, typhoon, and earthquake. Recently, in Japan, the frequency of short-time heavy rain has been increasing and the intensity of precipitation tends to be extremely strong. Precipitation has become localized, concentrated, and dramatically increased, causing flash flooding which result in a lot of damage to urban infrastructure. Heavy rains have caused a rapid land deformation, which causes the ground uplift -related disasters and damages to buildings[2]. In addition, extreme rainfall is expected to continue increasing due to the impact of climate change accompanying global warming[2]. Accordingly, the vulnerability of infrastructure due to heavy rain is an important urban problem, especially in densely populated areas. In the Tokyo metropolitan area where the recovery of groundwater level is remarkable, uplift pressure above the designed value and ground strain are generated in the underground facilities, and damage to the underground structures is recognized[3][4]. Widespread uplifting pressures and ground uplifting events due to the restoration of groundwater levels may gradually compromise the safety of underground facilities such as railways, roads, and communications networks that form the social infrastructure of large cities. It can also affect the safety and stability of the foundation of any structure. Using remote sensing technology to continuously monitor the deformation of wide range of land with high accuracy, it is possible to continuously monitor the ground uplift phenomenon and the stability of buildings. The short-term continuous land information data is required for a detailed analysis in Japan, and if this technology is properly verified, it is expected that it will be effectively utilized for the appropriate maintenance and renewal of infrastructure, including the design method of underground structures, in the future.

In this study, the long-term continuous land deformation (subsidence or uplift) analysis based on Consecutive Differential Interferometry Synthetic Aperture Radar (DInSAR) with the small spatial and short temporal baseline between satellites was carried out in Yokohama Yokosuka and Miura cities, Kanagawa prefecture, Japan. The satellite data used thirty-three pairs in descending orbit from December 27, 2017, to November 17, 2020; and twenty-two data pairs in

Corresponding author:
Katsunoshin Nishi (e-mail: katsunoshin.nishi@hotmail.com)
This paper was submitted on February 18, 2021; and accepted on March 9, 2021.

ascending orbit from June 26, 2019 to October 30, 2020, using Sentinel-1 C-band. The conventional Consecutive DInSAR used image pairs with large spatial and long temporal baseline between satellites for the purpose of estimating long-term land deformation[5]. However, since the purpose of this study is to observe the continuous land deformation in a short period, the temporal baseline was set at 12 days of Sentinel-1 revisiting time for analysis. Yokohama, Yokosuka and Miura cities were chosen as the subject of this research for the following considerations: Yokohama city can be characterized as an urban area, Miura city as a mountainous area, and Yokosuka city as an intermediate area between the urban and the mountainous areas in Kanagawa prefecture. The contrasting topographical environments of the three cities make the Consecutive DInSAR results of these cities useful in order to examine future versatility (of other city/area) in Japan. In addition, the analysis based on SAR for the land deformation has not been carried out in Kanagawa Prefecture of the Tokyo metropolitan area until now. Therefore, observation of land deformation in three cities using Consecutive DInSAR technique in this study is significant for future study of SAR utilization in Japan. To verify the Consecutive DInSAR data, the results were compared with the daily coordinate values (Ellipsoidal height) of the Global Navigation Satellite System (GNSS) ground control points operated by the Geographical Survey Institute (GSI).

Thus, this research aims to monitor the long-term continuous land deformation (subsidence or uplift) in Yokohama, Yokosuka, and Miura cities in Kanagawa prefecture using Sentinel-1 C-band Consecutive DInSAR technique with the small spatial and short time baseline between satellites. We believe that the study results will be useful as scientific information for the government officials to consider policy planning to minimize the impact of land deformation and stability of underground infrastructure.

II. Materials

A. *Satellite Dataset*

The satellite data comprises of thirty-three Sentinel-1 data pairs in descending orbit (relative orbit number 46) and twenty-two Sentinel-1 data pairs in ascending orbit (relative orbit number 39) as shown in Table 1. The polarization is VV (vertical transmit and vertical receive) with incident angle 38.3°. Only data with smaller spatial baseline and temporal baseline were chosen for this research with the maximum temporal baseline and spatial baseline 96 days and 142 m, respectively in the descending orbit and the maximum temporal baseline and spatial baseline 72 days and 131 m, respectively in the ascending orbit. The time baseline for the analysis was set at a few months according to the four seasons in Japan. However, after April 2020, the satellite images were acquired at a period of 12 days in order to obtain more precise data of land deformation because the short-term continuous land information data is required for more detailed analysis in Japan.

GNSS control points were used to validate the land deformation results obtained by adopted technique. GNSS control points are composed of Yokohama city (GNSS ID: 93032), Yokosuka city (GNSS ID: 93067) and Miura city (GNSS ID: 960759) in Kanagawa prefecture and Futtsu city (GNSS ID: 93036) in Chiba prefecture. The vertical fluctuation of each GNSS control point was observed by adopting Futtsu control point as reference point. Table 2 shows the location data of GNSS control points in Yokohama, Yokosuka, Miura, and Futtsu cities.

III. Methods

A. *Consecutive DInSAR technique*

Consecutive DInSAR in this study is a method for selecting a pair of small spatial baselines and short temporal baselines (master image and slave image) and alternately changing the master image and the slave image over a continuous period of time. By selecting smaller spatial baselines and shorter temporal baselines, the continuous fluctuation can be appropriately extracted while minimizing the effect of spatiotemporal interference[6]. In this process, one image is labeled as a master image, another is the slave image, and the process is repeated in consecutive periods for long-term continuous monitoring of land deformation as shown in Figure 1.

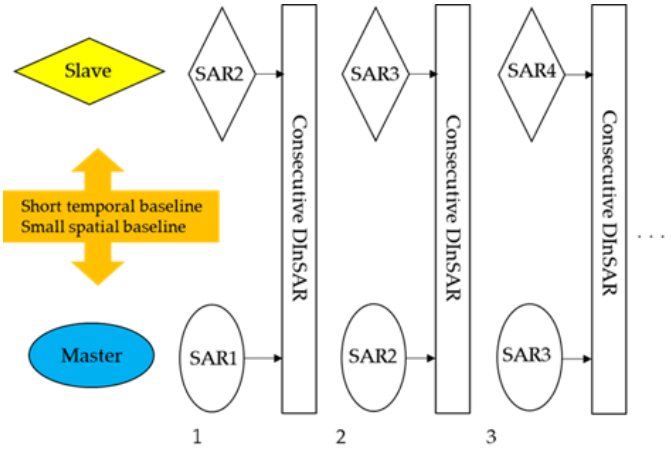

Figure 1 Consecutive DInSAR process

Traditional InSAR methods are Persistent Interferometric SAR (PSI-SAR)[7] and Small Baseline Subset (SBAS)[8] methods, which can track topographic changes in time series with high accuracy. However, PSI-SAR analyzes only point scattering (PS) with high phase accuracy and removes pixels with low coherence, therefore it cannot be used effectively in mountainous areas with few PS pixels[9]. Also, SBAS can be used in mountainous areas with the use of distributed scattering (DS) points, but since it discards the pixels with low coherence in order to suppress errors in phase continuity, the applicable range in mountainous areas is limited[9]. On the other hand, Consecutive DInSAR can use the pixels with low coherence that are removed in PSI-SAR and SBAS methods, therefore it has the potential to estimate the land deformation in mountainous area with high accuracy. This technique is expected to be useful in the field of disaster monitoring and environmental change measurement where continuous observation is strongly required.

Table 1 Sentinel-1 C band data pairs

Pair No.	Orbit	Acquisition date (YY/MM/DD)	Temporal Baseline (days)	Spatial Baseline (meter)
1	Descending	2017/12/27-2018/02/13	48	127
2		2018/02/13-2018/05/20	96	110
3		2018/05/20-2018/07/07	48	27
4		2018/07/07-2018/09/05	60	94
5		2018/09/05-2018/11/16	72	32
6		2018/11/16-2019/01/27	72	34
7		2019/01/27-2019/03/16	48	50
8		2019/03/16-2019/05/03	48	121
9		2019/05/03-2019/06/20	48	133
10		2019/06/20-2019/07/14	24	47
11		2019/07/14-2019/08/07	24	5
12		2019/08/07-2019/10/06	60	24
13		2019/10/06-2019/11/11	36	58
14		2019/11/11-2019/12/05	24	103
15		2019/12/05-2020/01/10	36	140
16		2020/01/10-2020/02/15	36	142
17		2020/02/15-2020/03/22	36	123
18		2020/03/22-2020/04/03	12	86
19		2020/04/03-2020/04/15	12	32
20		2020/04/15-2020/04/27	12	15
21		2020/04/27-2020/05/09	12	28
22		2020/05/09-2020/05/21	12	69
23		2020/05/21-2020/07/08	48 (※)	64
24		2020/07/08-2020/07/20	12	87
25		2020/07/20-2020/08/01	12	34
26		2020/08/01-2020/08/13	12	90
27		2020/08/13-2020/08/25	12	21
28		2020/08/25-2020/09/06	12	20
29		2020/09/06-2020/09/30	24 (※)	13
30		2020/09/30-2020/10/12	12	30
31		2020/10/12-2020/10/24	12	52
32		2020/10/24-2020/11/05	12	54
33		2020/11/05-2020/11/17	12	21

※ The June and September in 2020 was omitted because of the unusually high precipitation.

Pair No.	Orbit	Acquisition date (YY/MM/DD)	Temporal Baseline (days)	Spatial Baseline (meter)
1	Ascending	2019/06/26-2019/08/13	48	26
2		2019/08/13-2019/10/24	72	24
3		2019/10/24-2019/11/17	24	62
4		2019/11/17-2019/12/11	24	131
5		2019/12/11-2020/01/16	36	56
6		2020/01/16-2020/02/21	36	8
7		2020/02/21-2020/03/28	36	33
8		2020/03/28-2020/04/09	12	8
9		2020/04/09-2020/04/21	12	31
10		2020/04/21-2020/05/03	12	33
11		2020/05/03-2020/05/15	12	71
12		2020/05/15-2020/05/27	12	47
13		2020/05/27-2020/06/08	12	49
14		2020/06/08-2020/07/02	24(※)	36
15		2020/07/02-2020/07/14	12	90
16		2020/07/14-2020/08/07	24	21
17		2020/08/07-2020/08/19	12	93
18		2020/08/19-2020/08/31	12	88
19		2020/08/31-2020/09/24	24(※)	69
20		2020/09/24-2020/10/06	12	70
21		2020/10/06-2020/10/18	12	130
22		2020/10/18-2020/10/30	12	25

※ The June and September in 2020 was omitted because of the unusually high precipitation.

Table 2 Location data of GNSS control points used in the research

No	City	Latitude	Longitude	GNSS ID
1	Yokohama	35°26′11″.3445N	139°39′13″.5005E	93032
2	Yokosuka	35°26′70″.9340N	139°66′48″.3807E	93067
3	Miura	35°09′39″.1213N	139°36′49″.8382E	960759
4	Futtsu	35°31′17″.0188N	139°82′55″.2063E	93036

The analysis of Consecutive DInSAR was done in SARPROZ software provided by preiZ[10]. The Digital Elevation Model (DEM) was acquired from the Shuttle Radar Topography Mission (SRTM) with a grid resolution of 30 m (1 arcsecond) and was used with accurate satellite orbital data in order to eliminate the height phase and flat earth phase differences. Also, filters by Goldstein Werner were applied to reduce phase noise. Finally, phase unwrapping was performed to derive the real value of land deformation, and the result was geocoded into google earth.

B. *GNSS control point*

In Japan, GNSS Earth Observation Network System (GEONET) is managed and operated by GSI for monitoring crustal deformation[11]. The whole Japan is covered by approximately 1,300 nationwide GEONET stations at about 20 km distance to each other. These GEONET stations measure the amount of daily land surface fluctuations. GEONET uses ITRF2005 as a reference coordinate frame and GRS80 as reference ellipsoid[12]. The daily coordinated value of the GNSS point is calculated by GPS data and were analyzed using Bernese Ver.5[13]. The resultant data contains geocentric coordinate values, latitude, longitude, and ellipsoidal height. The accuracy of ellipsoidal height is approximately 1 cm[14].

Also, the GNSS data may have the following coordinate changes for the causes other than crustal deformation; Seasonal changes due to water vapor, trees, and groundwater, Data steps due to antenna replacement and tree felling, Slow change due to pillar inclination, Jump and Dispersion due to frontal passage and surrounding work, and Vertical amplitude due to radio interference , so attention should be paid when analyzing the data[15]. Japan has four seasons in a year and groundwater is pumped up more often in summer. Therefore, the GNSS control point is characterized by a seasonal change in which the ellipsoidal height occurs from around May to August every year, and also, the ellipsoidal height rises slowly from around September to the next spring. This is caused by not a crustal movement but a seasonal change[15].

IV. Study Area

A. *Location and Geological Information*

The study area chosen for this research consists of Yokohama, Yokosuka and Miura cities in Kanagawa prefecture, Japan as shown in Figure 2. The square red lines are observation areas captured in descending and ascending orbits. The GNSS control points are shown in yellow green circle. Also, the geology map of Yokohama, Yokosuka and Miura cities is shown in Figure 3. In this study, we defined Yokohama city as the central area (Population: more than 1 million), Miura city as the mountainous area (Population: 0.1 million or less), and Yokosuka city as the middle area between the urban area and the mountainous area based on the following regional characteristics.

Yokohama city is the center of economic activity in the Tokyo metropolitan area, with densely packed commercial and residential buildings. It is also the government-designated city with 18 administrative districts in Kanagawa prefecture. The location is at the longitude of 139° 27'52" -139° 43'31" E, and latitude of 35° 18'45" -35° 35'34" N. The city population is the largest in Japan (3.75 million), and the area is most extensive in Kanagawa Prefecture (475 km^2). The area of GNSS point (93032) is called as "YATO" which is a landscape unit where flat land takes the shape of a horseshoe, cutting into hilly regions[16] and the altitude is 19.1 m[17]. The base of the terrace where it is located is mudstone or sandy mudstone of the Kazusa Group from Neogene Pliocene to the early Pleistocene. On top of that, there are three layers of soil: the sandbank layer, which forms the Sagami Group from the middle to late Pleistocene, the Shimosueyoshi layer, which mainly consists of mud layers, and the Kanto loam layer, which is composed of volcanic ashy clay soil. The sandy and gravelly soils of the Kazusa Formation, the sandy soils of the Sagami Group, and the gravelly soils of the Shimosueyoshi Formation are highly permeable and are prone to land subsidence as the groundwater level decreases. Also, the loam layer is generally characterized by high resistance to water infiltration, but becomes soft when it contains moisture[3]. According to a boring survey in Yokohama city, the area of 93032 is composed of embankments composed of sand and gravel up to a depth of 5.7 m, organic clay from 5.7 to 7.8 m, and sandy mudstone from 7.8 to 11.37 m[18]. The geology of Yokohama city is that the alluvium consisting mainly of cohesive soil is deposited thickly on the upper part of diluvium, and the ground is soft.

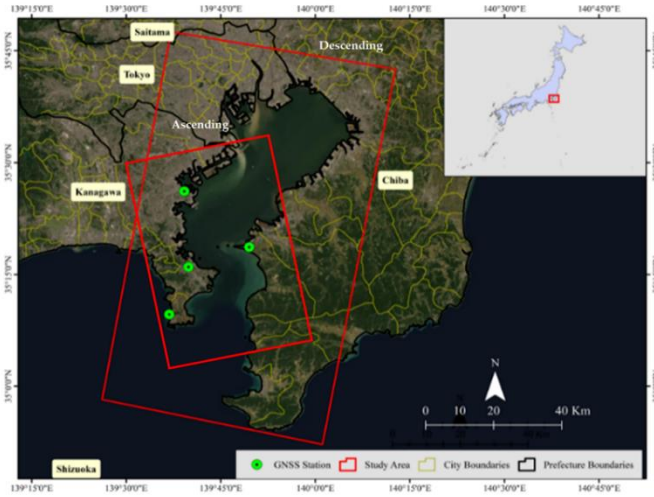

Figure 2 The study area (Yokohama, Yokosuka, and Miura cities in Kanagawa prefecture)

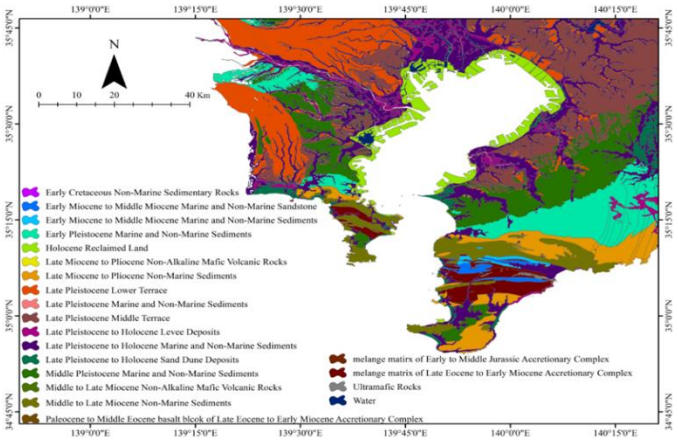

Figure 3 Geology Map in Kanagawa prefecture (The Geological Survey of Japan[21])

Yokosuka city is also designated as a core city in Kanagawa prefecture. It covers most of the Miura Peninsula in southeastern Kanagawa Prefecture, which are composed of many mountainous areas, hilly areas, and few flatlands. The location is at the longitude of 139° 34'34"-139° 44'48" E and latitude of 35° 11'24"-35° 19'50"N. Also, there are many tunnels due to the mountainous terrain. The center of the city is crowded with large factories and houses, and there is a lot of

nature along the coast and agriculture is thriving. The population is 0.40 million, which accounts for around 4.3% of the population of Kanagawa Prefecture and the area is about 100 km^2, which is around 4.2% of Kanagawa Prefecture. The area of GNSS point (93067) is consists of the Zushi Formation of the Miura Group deposited from the late Miocene to the late Pliocene[19]. The Zushi Formation consists mainly of alternating layers of mudstone and sandstone and intercalates thin layers of tuff and the basal part is accompanied by tuffaceous sandstone and conglomerate[19].

In addition, Miura city is located at the southernmost tip of the Miura Peninsula, which is occupied by a plateau at an altitude of 40 m to 60 m and is also surrounded by Tokyo Bay and Sagami Bay. The location is at the longitude ranging between 139° 36'10"-139° 40'55" E and latitude ranging from 35° 07'44" to 35° 12'35" N. It has the second least populous city (0.04 million), and the area is smaller in Kanagawa prefecture (32 km^2). The area where GNSS point (960759) is located in a loam plateau made of volcanic ash clay on top of the Miura Group composed of siltstone and scoria. The loam soil and the silt rocks and scoria of the Miura Group have low permeability and stable ground. According to the boring survey by Kanagawa prefecture, the soil consists of organic loamy soil up to a depth of 0.5 m, gravelly loam from 0.5 to 2.9 m, fine sand from 2.9 to 3.2 m, and tuffaceous sandstone composed of scoria gravel from 3.2 to 14.0 m[20]. Besides, the land of Miura city is uplifted every year. The Miura Peninsula is located in the area of the Sagami Trough, where the Philippine Sea Plate is subducted beneath the Eurasian Plate, and several active faults (The Miura Peninsula Fault Group) are distributed.

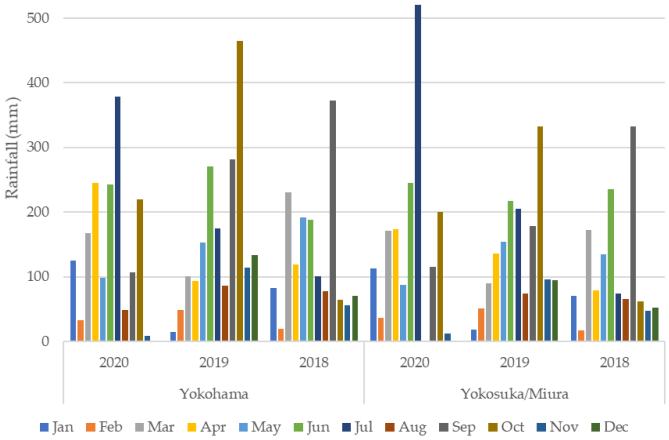

Figure 4 The rainfall intensity distribution in Kanagawa prefecture (Yokohama, and Yokosuka/Miura cities)

B. *Precipitation Information*

Figure 4 presents the rainfall intensity distribution of Yokohama, Yokosuka, and Miura cities from 2018 to November 2020[22]. Statistically, raindrops start in May and June and then slow down during the summer season, and more rainfalls restart in September and October. Typhoons are particularly common in September. Figure 4 shows that there is no particular significant difference in precipitation amount between Yokohama and Yokosuka/Miura cities. Also, in 2020, the precipitation amount was almost large in the cities, and especially in April, it was 174 mm/month in Yokohama city and 245 mm/month in Yokosuka/Miura city, respectively. Also, monthly rainfall intensity in Yokohama, Yokosuka, and Miura cities was highest in July 2020 (520 mm/month) and lowest in August 2020 (1mm/month) in Yokosuka, and Miura cities.

V. Results

A. *Land displacement map on Consecutive DInSAR*

In this Consecutive DInSAR analysis, the satellite line-of-sight (LOS) variability values of Yokohama, Yokosuka and Miura cities were measured using Futtsu city as a reference point and then the LOS values were converted to vertical values. For the validation, the Consecutive DInSAR results in Yokohama, Yokosuka, and Miura cities were compared with the ellipsoidal elevation data of each GNSS point in the consecutive period. Similarly, in the GNSS data processing, the vertical variation values of Yokohama, Yokosuka and Miura cities were analyzed using Futtsu city as the fixed point. In calculating the fluctuation value from the GNSS data, the GNSS data for a total of 11 days for 5 days before and after the observation date of the SAR data was used to obtain the mean value and standard deviation of the fluctuation for 11 days at each GNSS point. In our analysis, the location of the GNSS points did not necessarily coincide with the site of the DInSAR, but we assumed that the surface variability is uniform at 50 m around the GNSS points and estimated the timeseries variability.

Figure 5 and Figure 6 are the representative examples selected from Table 1 of coherence and land displacement maps of descending and ascending orbits, respectively, which clearly show the land uplift and subsidence. Figure 5 is the coherence and land displacement maps of the descending orbit from July 7, 2018 to September 5, 2018, and Figure 6 is those of the ascending orbit from November 17, 2019 to December 11, 2019. If the normal baseline is small and the temporal baseline is short, the interface expected to be created is accurate[23]. Based on the interferogram image, the process of flattening, DEM removal, and unwrap are done, and the final result is the land deformation map[23]. From these figures, it can be seen that the coherence in the research area is high, which means high cross-correlation between the two pairs in each descending and ascending orbit. Also, the land displacement maps in these figures show the relativeness of land displacement in color, with red indicating subsidence and blue indicating uplift.

In accordance with the above research procedure, SAR images of the other data pairs in Table 1 were acquired and land displacement values were acquired from the land deformation maps. However, obtaining these land displacement maps is not in itself part of the main aim of this paper. Instead, we intend to compare the land displacement values from Consecutive DInSAR results and GNSS data and prove the validity of the Consecutive DInSAR technique with the small spatial and short time baseline between satellites. Nevetheless, for completeness and in order not to divert the reader's attention from our processing, we provide the all the land deformation maps of descending and ascending orbits in Table 1 in Appendix.

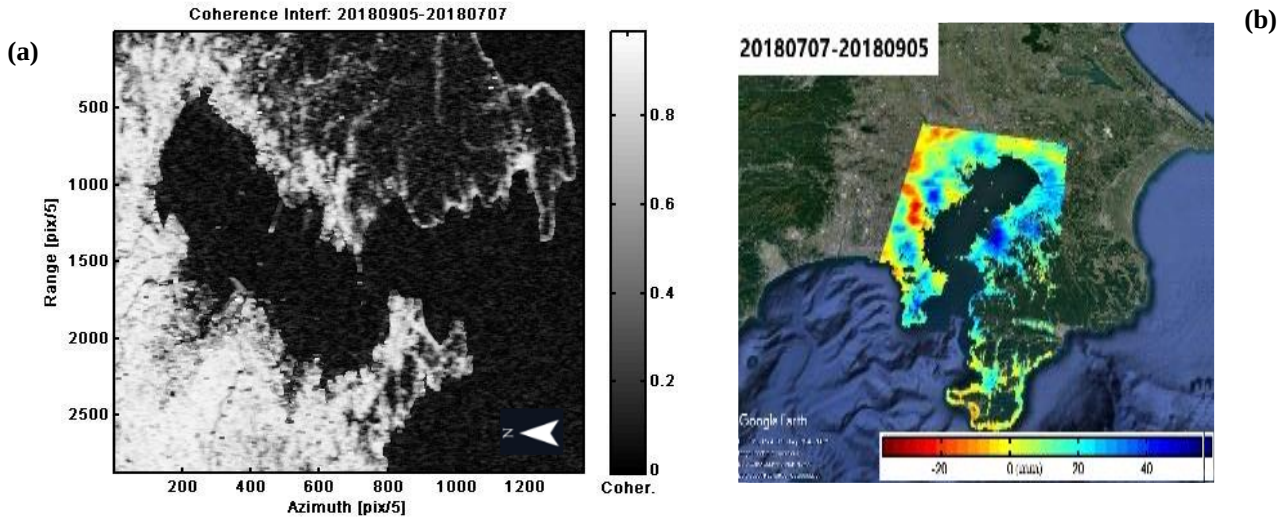

Figure 5 Land displacement map in descending orbit based on Consecutive DInSAR processing: (a) Coherence image; (b) land displacement map of this research area

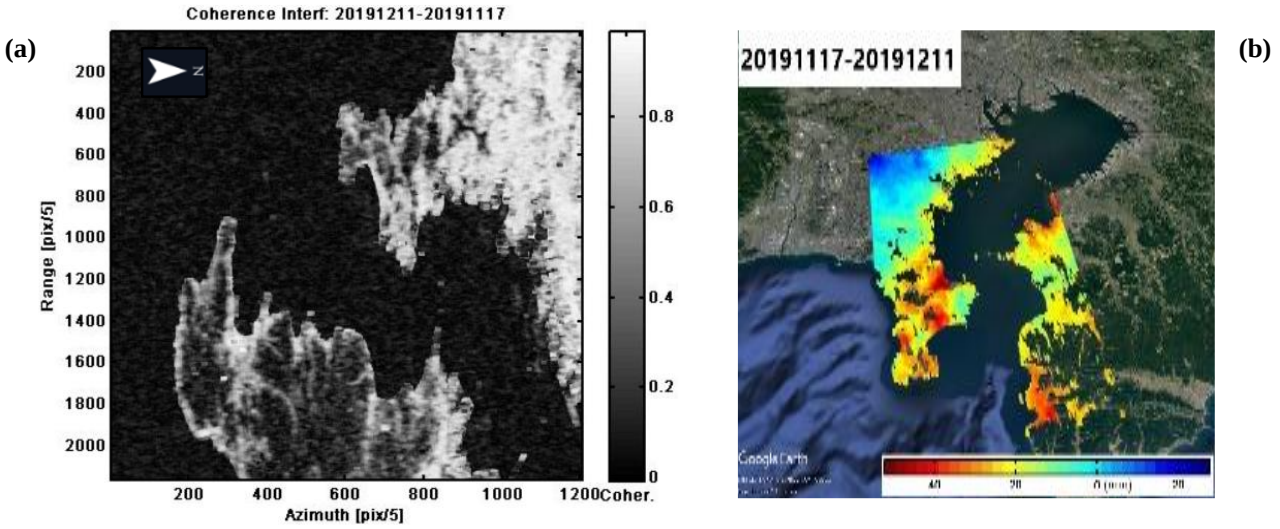

Figure 6 Land displacement map in ascending orbit based on Consecutive DInSAR processing: (a) Coherence image; (b) land displacement map of this research area

B. Comparison with Consecutive DInSAR results, and GNSS data

Generally, SAR interferograms contain several noise sources, such as atmosphere noise, and ionosphere noise. In order to reduce these errors, the Consecutive DInSAR performed filtering and multi-look processing (5×5), but it is still considered to have residual errors in these displacement maps. Therefore, in order to obtain the data which further reduced these noises from the Consecutive DInSAR results, we used the stacking method in which the added SAR interferometry results were divided by the sum of the periods. Adding multiple data improves the S/N ratio by reducing temporally random errors due to changes in the ionospheric electron density and water vapor distributions[24]. In stacking method, the amount of data is an important factor for improving accuracy, but it is said that the effect of reducing errors can be confirmed even if the data used is about three pairs[24]. Therefore, in this study, we performed it using three pairs of continuous data for noise reduction. Figure 7 and Figure 8 show line graphs of displacement map data for Yokohama, Yokosuka and Miura cities, to which the above stacking method is applied. It is found that the Consecutive DInSAR results for three cities have a similar tendency with each GNSS data.

In order to evaluate the coincidence of the time series fluctuation between the Consecutive DInSAR data and the GNSS data in Yokohama, Yokosuka and Miura cities, RMSEs for three cities were calculated. As a result, the RMSEs in descending orbit were 0.41 cm for Yokohama city, 0.49 cm for Yokosuka city, and 0.49 cm for Miura city and the RMSEs in ascending orbit were 0.68 cm for Yokohama city, 0.53 cm for Yokosuka city, and 0.58 cm for Miura city. Here, an error bar of standard deviation is added to the GNSS data of the three cities in Figure 7 and Figure 8. It can be found that the displacements of the Consecutive DInSAR in three cities on the ascending and descending orbits were within 1 cm of GNSS data accuracy.

Figure 7 Comparison of Consecutive DInSAR results and GNSS data in descending orbit: (a) Yokohama, (b) Yokosuka, (c) Miura

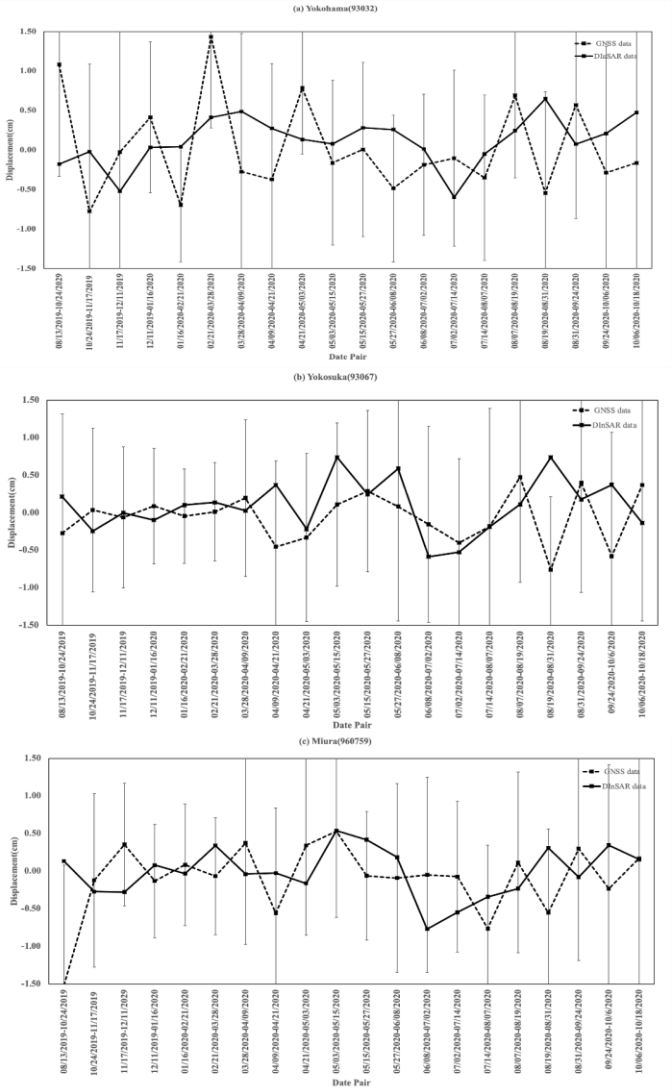

Figure 8 Comparison of Consecutive DInSAR results and GNSS data in ascending orbit: (a) Yokohama, (b) Yokosuka, (c) Miura

The graph in descending orbit (Figure 7) shows that the land uplift is remarkable in May to early July 2018. Similarly, the graph in ascending orbit (Figure 8) shows that the land uplift occurred in May to June 2020. Generally, the land uplift is caused by seasonal groundwater recovery and interplate subduction. The land uplift occurs in the timing with rainy season, which is in May and June called "Tsuyu" in Japan (Figure 7 and Figure 8). The effects of precipitation are related to the groundwater table, and the precipitation is correlated with the permeable layer[3][4]. Thus, land uplift is considered to be caused by seasonal recovery of groundwater because land uplift shows seasonal variations. In other words, it is considered that the shift from the dry season to the wet season resulted in the recovery of the groundwater level due to the increase in precipitation and the uplift of the land. Also, as a feature of the land in Yokohama city, the embankment and sandy soil of the Sagami group and Kazusa group are excellent in water permeability, and it is possible that the groundwater table will rise with the increase of rainfall. In fact, the land of Yokosuka and Miura cities is also considered to have risen from May to early July 2018, but the displacement amount was not as large as that in Yokohama city. The land of Yokosuka and Miura cities is considered to be less susceptible to the effect of precipitation because it is composed of impermeable Kanto loam layers and Miura group. Also, the graph in descending orbit (Figure 7) shows land subsidence is confirmed from July to early September 2018. In general, the causes of land subsidence include excessive pumping of groundwater, construction of peripheral facilities, shortage of artificial embankments, and liquefaction due to earthquakes. In Figure 7, the land subsidence occurred in the timing with the dry season, which is July and August in Japan and there are no reports of

construction of peripheral facilities or earthquakes in the period. The land displacement occurs because of the decrease in surface infiltration due to insufficient rainfall and a decrease in groundwater level due to increased groundwater use during the dry season in summer. Thus, it is considered that the lowering of the ground water level caused the compression by the consolidation of the clay layer and caused the land subsidence in Figure 7.

Moreover, we observed the annual land displacement velocity (cm/year) in the Miura Peninsula from Figure 7(c) and Figure 8(c). It is said that the Miura Peninsula has risen by several centimeters every year by crustal deformation by subduction of the Philippine Sea plate to the Eurasia plate[25]. In this analysis, linear fitting to Consecutive DInSAR data and GNSS data in Miura city was performed under the assumption that land changes at a constant rate to estimate the annual land displacement. The results show that the annual land displacement in descending orbit for Consecutive DInSAR results was -0.41 cm/year and that for GNSS data was -0.80 cm/year and the annual land displacement in ascending orbit was -0.71 cm/year and that for GNSS data was -0.60 cm/year. The Boso Peninsula, where Futtsu city is located, is also said to be a complex region where the Philippine Sea plate subducts into the North American plate and the Pacific plate into the Philippine Sea plate. The Boso Peninsula has crustal movement caused by the plate subduction[25]. The comparison of the annual land displacement between the Miura Peninsula and the Boso Peninsula shows that the Boso Peninsula may be more strongly affected by the upheaval of the plate than the Miura Peninsula.

VI. Discussion

For the cities of Yokohama, Yokosuka, and Miura, the following can be seen from Figure 7 and Figure 8. The Consecutive DInSAR results are included in the error range of GNSS data, but it can be seen that there are some differences in these line graphs. The reduction of the error was carried out as described in Section V.B, but since the research area is an urban area, it is considered that the noise by multiple scattering could not be reduced completely. As a future task, it is necessary to develop a processing method of multiple scattering in urban areas. Furthermore, GNSS control points can detect the land deformation at the installation site, but cannot observe the displacement around it. On the other hand, Consecutive DInSAR can detect the land deformation in a plane, so it can observe the displacement in a plane that GNSS control points cannot detect. These differences appear in the differences between GNSS data and Consecutive DInSAR results.

Also, in this study, we used Sentinel-1 C-band data, which is free of charge and has high resolution, however, they are reflected by the leaves during the summer season when the leaves grow thickly because the C-band data are a short wavelength and the accuracy in summer decreases. In order to suppress the influence of trees and to improve the accuracy during summer, it is possible to transmit radio waves through vegetation by utilizing the L-band with a long wavelength. ALOS-2 PALSAR is said to be very useful in the coherence of vegetation areas and as a future study, we would like to conduct an analysis comparison using the L-band and C-band.

In addition, although Kanagawa Prefecture (Yokohama, Yokosuka and Miura cities) was the subject of this study, since positive results were obtained from the Consecutive DInSAR map, we would like to expand it to the Kanto region, including Chiba Prefecture and Tokyo, where there is a risk of many typhoons, heavy rains in the future. Also, as a field study, we will conduct an experiment using an aircraft equipped with C-band SAR and compare the analysis accuracy with the results of this paper.

VII. Conclusions

It can be confirmed that Consecutive DInSAR results are consistent with GNSS data. The RMSEs in descending orbit for Yokohama, Yokosuka and Miura cities were estimated to be 0.41 cm 0.49 cm and 0.49 cm, respectively. Also, the RMSEs in ascending orbit for these cities were 0.68 cm, 0.53 cm, and 0.58 cm, respectively. These RMSEs are within the accuracy of GNSS data. The Consecutive DInSAR analysis used in this study demonstrate its capability to analyze the land displacement monitoring over under different topographical conditions. Similarly, the causes of land uplift and subsidence during each observation period were discussed from the viewpoint of seasonal variation and land characteristics in Japan. In Yokohama city where there are many high-rise buildings, if the groundwater level is considered while designing underground structures, the land deformation issue can be addressed in appropriate manners. The accuracy of Consecutive DInSAR analysis depends on the number of SAR data, the type of satellite data, and the region to be analyzed, but in this analysis, we were able to estimate land deformation in Yokohama, Yokosuka and Miura cities with sub-centimeter accuracy/year using the Sentinel-1 C-band data.

In this study, we could verify the validity of the method of Consecutive DInSAR in small spatial and short temporal baseline. The Consecutive DInSAR method is expected to be applicable in the future in the field of disaster monitoring where high accuracy observation over a wide area is required in consecutive time.

Acknowledgments

The authors would like to thank SARPROZ team for providing software license for this research, European Space Agency for Sentinel-1 data. Also, we would like to express our gratitude to Kaori Nishi and Noriko Nishi of Bella Earther company for their great support in this research.

Appendix

Figure A-1 shows land displacement maps in descending and ascending orbits for all data pairs in Table 1. Figure A-1 are the land displacement maps in the descending data pair of Table 1, and also, Figure A-2 are all land displacement maps in the ascending data pair of Table 1. Note that the land displacement map units are expressed in millimeters, and the legend varies for each map.

Figure A-1 Land displacement map in descending orbit based on Consecutive DInSAR processing (unit: mm)

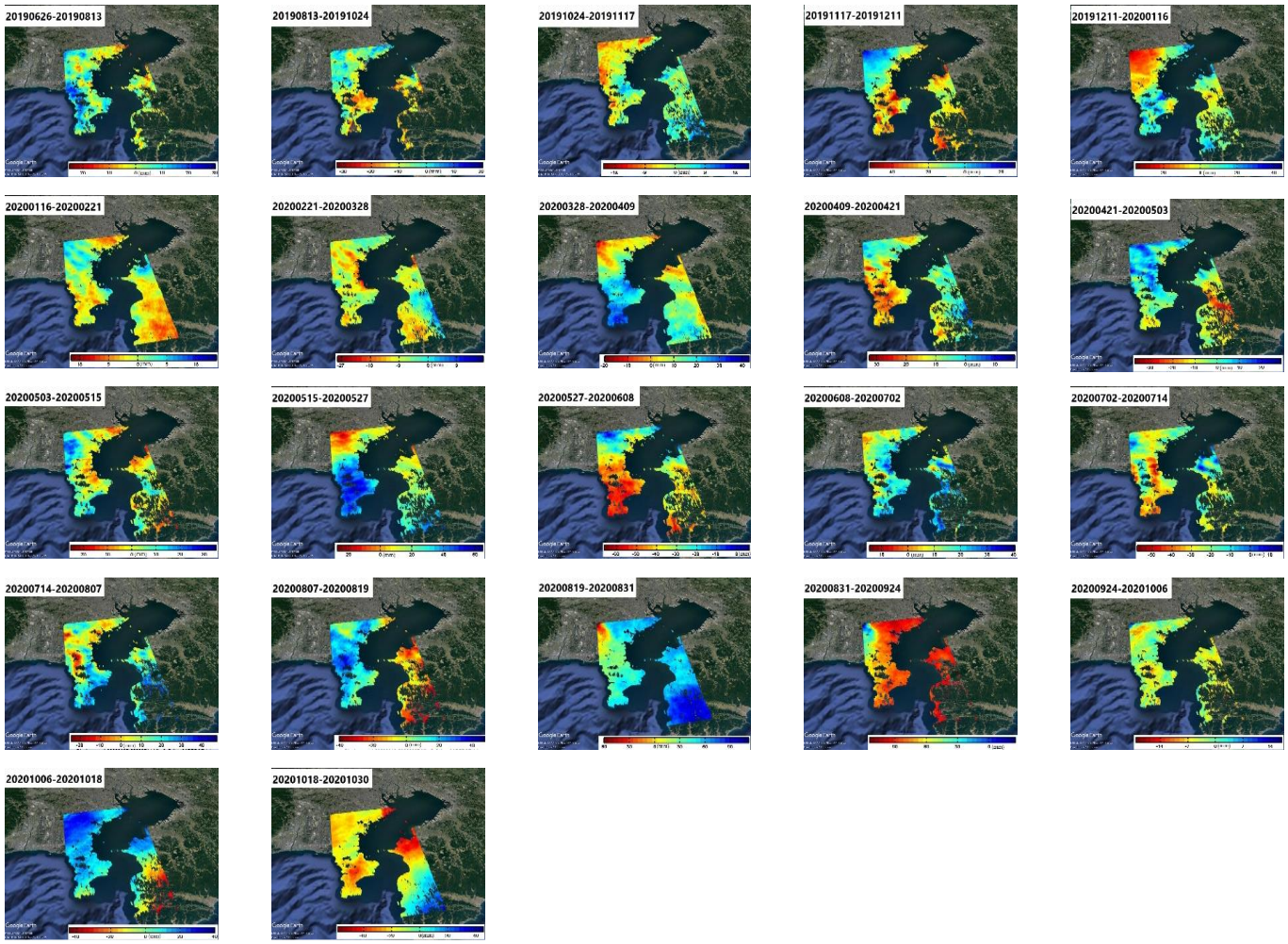

Figure A-2 Land displacement map in ascending orbit based on Consecutive DInSAR processing (unit: mm)

REFERENCES

[1] The National Institute of Population and Social Security Research. *Results of age-specific population projection (total, 0–14, 15–64, 65+, and 75+) for 2015–2045*; The National Institute of Population and Social Security Research, Tokyo, Japan, 2018.

[2] The Ministry of Land, Infrastructure, Transport and Tourism. *National Spatial Strategy*; The Ministry of Land, Infrastructure, Transport and Tourism, Tokyo, Japan, 2015.

[3] T. Kisanuki, M. Nishigaki, S.Noda, and T. Yamashita,"A Method of Determining The Groundwater Level for Design of Underground Stracture in The Geological Region Around Tokyo," *J. JSCE*, vol. 57, pp. 167–176, 2002.

[4] T. Kusaka et al, "Study on ground upheaval caused by the rise in groundwater level by centrifuge tests," *Japanese Geotechnical Journal*, vol. 6, no. 3, pp. 439–454, 2011.

[5] J. T. Sri Sumantyo, M. Shimada, P. P. Mathieu, and H. Z. Abidin,"Long-term consecutive DInSAR for volume change estimation of Land deformation," *IEEE Trans Geosci Remote Sens*., vol. 50, no. 1, pp. 259–270, 2012.

[6] P. Razi, J. T. S. Sumantyo, D. Perissin, H. Kuze, M. Y. Chua, and G. F. Panggabean, "3D land mapping and land deformation monitoring using persistent scatterer interferometry (PSI) ALOS PALSAR: Validated by Geodetic GPS and UAV," *IEEE Access*, vol. 6, pp. 12395–12404, 2018.

[7] A. Ferretti, C. Prati, and F. Rocca, "Permanent scatterers in SAR interferometry," *IEEE Trans Geosci Remote Sens*, vol. 39, no. 1, pp. 8–20, 2001.

[8] P. Berardino, G. Fornaro, R. Lanari, and E. Sansosti, "A new algorithm for surface deformation monitoring based on small baseline differential SAR interferograms," *IEEE Trans Geosci Remote Sens*, vol. 40, no. 11, pp. 2375–2383, 2002.

[9] T. Kobayashi.; Y. Morishita.; and S. Yamada. A Prototype System for InSAR time series analysis; The Geographical Survey Institute, Tokyo, Japan, 2018; pp.123-133.

[10] J. Widodo *et al.*, "Land subsidence rate analysis of Jakarta Metropolitan Region based on D-InSAR processing of Sentinel data C-Band frequency," *J. Phys. Conf. Ser*, vol. 1185, no. 1, 2019.

[11] H. Munekane. On Improving Precision of GPS-derived Height Time Series at GEONET Stations; The Geographical Survey Institute, Tokyo, Japan, 2013; pp.39-46.

[12] T. ElGharbawi and M. Tamura, "Measuring deformations using SAR interferometry and GPS observables with geodetic accuracy: Application to Tokyo, Japan," *ISPRS J. Photogramm. Remote Sens*, vol. 88, pp. 156–165, 2014.

[13] H. Nakagawa, T. Toyofuku, and K. Kotani, "Development and validation of GEONET new analysis strategy (version 4)," *J. Geogr. Surv. Inst*, vol. 118, pp. 1–8, 2009.

[14] Crustal Movement Reevaluated from Solutions of GEONET New Analysis Strategy (Ver.4):
Available online: https://www.gsi.go.jp/common/000054720.pdf (accessed on April 2, 2020).

[15] Geospatial Information Authority of Japan: Causes and characteristics of coordinates changes other than crustal movement.
Available online: https://www.gsi.go.jp/top.html (accessed on November 17, 2020).

[16] T. Mikasa, T. Uchihara, T. Shigemura, T.Tanaka and Y. Yamazaki, "A Study on Topographical Characteristic and Land Use Feature in 'Yato,'" *J Archit Plann Res*, vol. 80, no. 714, pp. 1825–1832, 2015.

[17] The Geographical Survey Institute: Elevation of observation point. Available online: https://www.gsi.go.jp/johofukyu/hyoko_system.html. (accessed on September 17, 2020).

[18] Geology view of Yokohama city. Available online: https://wwwm.city.yokohama.lg.jp/yokohama/Portal (accessed on September 17, 2020).

[19] The Geological Survey of Japan: Geology of Yokosuka city area: Available online: https://www.gsj.jp/data/50KGM/PDF/GSJ_MAP_G050_08084_1998_D.pdf (accessed on November 17, 2020).

[20] Geology view of Miura city. Available online: http://www.kanagawa-boring.jp/boring/index.htm(accessed on November 17, 2020).

[21] The Geological Survey of Japan: Geology map of Kanagawa prefecture. Available online: https://www.gsj.jp/en/ (accessed on November 17, 2020).

[22] Japan meteological agency: Precipitation information of Kanagawa prefecture: Available online: https://www.jma.go.jp/jma/indexe.html. (accessed on November 17, 2020).

[23] J. Widodo *et al.*, "Application of SAR interferometry using ALOS-2 PALSAR-2 data as precise method to identify degraded peatland areas related to forest fire," *Geosci*, vol. 9, no. 11, pp. 1–15, 2019.

[24] M. Yamanaka, Y. Morishita, and Y. Osaka, "Detection of ground subsidence by InSAR time series analysis," *J. Geod. Soc. Japan*, vol. 49, no. 1, pp. 1–23, 2003.

[25] A. Hasegawa, J. Nakajima, N. Uchida, and N. Umino, "Subduction of Two Oceanic Plates and Unique Seismic Activity beneath the Tokyo Metropolitan Area," *J Geog* , vol. 122, no. 3, pp. 398–417, 2013.

[26] Geospatial Information Authority of Japan: Error of the interferometric SAR. Available online: https://www.gsi.go.jp/uchusokuchi/sar_error.html.(accessed on December 29, 2020).

[27] P. Razi, J. T. S. Sumantyo, K. Nishi, J. Widodo, A. Munir, and F. Febriany, "Effect of Earthquake Intensity to Land Deformation Observed from Space," *Prog. Electromagn. Res. Symp.*, vol. 2019-June, pp. 2123–2128, 2019.

[28] A. Moreira, P. Prats-Iraola, M. Younis, G. Krieger, I. Hajnsek, and K. P. Papathanassiou, "A tutorial on synthetic aperture radar," *IEEE Trans.Geosci. Remote Sens*, vol. 1, no. 1, pp. 6–43, 2013.

[29] R. F. Putri, L. Bayuaji, J. T. S. Sumantyo, and H. Kuze, "Terrasar-X DInSAR for land deformation detection in Jakarta Urban area, Indonesia," *J. Urban Environ. Eng.*, vol. 7, no. 2, pp. 195–205, 2013.

[30] Geology view of Yokosuka city. Available online: https://www.gsi.go.jp/johofukyu/hyoko_system.html. (accessed on September 17, 2020).

[31] K. Ishitsuka, T. Matsuoka, "Accuracy Evaluation of Persistent Scatterer Interferometry Using ALOS/PALSAR Data:A Case Study of Surface Displacement in the Kujukuri Plain, Chiba Prefecture," *J. Remote Sens. Soc. Japan*, vol. 36, no. 4, pp. 328–337, 2016.

[32] H. Iwaki et al. Deformation and analysis and trial study for structural monitoring using C-band SAR imaging satellite for 2016 Kumamoto. *J. JSCE*, vol. 73, no. 4, p. I_1018-I_1023, 2017.

[33] Y. Morishita. Reduction of Spatially Long Wavelength Noises in SAR Interferograms Using GNSS Data. *Journal of the Geodetic Society of Japan*, vol. 62, no. 2, pp. 89–100, 2016.

[34] J. Tetuko *et al.*, "Analysis of Coastal Sedimentation Impact to Jakarta Giant Sea Wall Using PSI ALOS PALSAR," *IEEE Geosci. Remote Sens. Lett.*, vol. 13, no. 10, pp. 1472–1476, 2016.

[35] Katsunoshin Nishi, J. T. S. Sumantyo, Mirza Muhammad Waqar, Chen Xiangping, Ramadan Gamal, "Accuracy Verification of Consecutive DInSAR and PSI-SAR Using GNSS Data" *IEICE Technical Report*, vol.120, no. 250, pp.13-18, 2020.